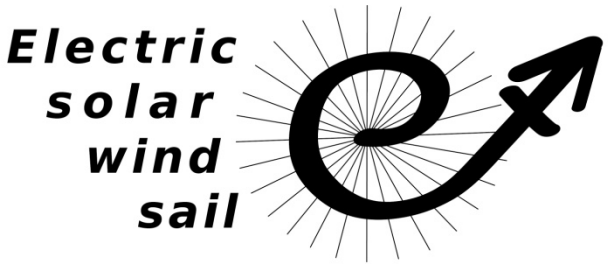

ESAIL D21.3
Tether factory (1 km) design, implementation and production

Work Package: **WP 21**

Version: **Version 1.0**

Prepared by: University of Helsinki, Henri Seppänen

Date: Helsinki, May 27th, 2013

Approved by: University of Helsinki, Edward Hæggström

(List of participants:)

Participant no.	Participant organisation	Abbrev.	Country
2	University of Helsinki	UH	Finland

Note: This text is submitted for publication in Review of Scientific Instruments in May 17th 2013.

Table of Content

Abstract

We produced a 1 km continuous piece of multifilament electric solar wind sail tether of 25-50 μm-diameter aluminum wires using a custom made automatic tether factory. The tether comprising 90704 bonds between 25 and 50 μm diameter wires is reeled onto a metal reel. The total mass of 1 km tether is 10 g. We reached a production rate of 70 m/24 hours and a quality level of 1 ‰ loose bonds and 2 ‰ rebonded ones. We thus demonstrated that production of long electric solar wind sail tethers is possible and practical.

1. Introduction

The electric solar wind sail (E-sail) is a propellantless space propulsion invention for interplanetary missions [1]. Propellantless space travel which is free from the limitations set by the rocket equation holds promise for scientific exploration and commercial utilization of the solar system [2] [3] [4]. Space sails permit long range exploration, and in many cases also returning at reasonable cost. The E-sail tethers must be electrically conducting, lightweight, sufficiently strong, and resistant to micrometeoroids. We have previously shown that the E-sail concept can be realized using ultrasonic Al-wire bonding technology [5]. This technology allows light and strong meteoroid resistant four-wire Heytether structures of suitable size to be built in an automated factory [6].

The core of the structure is the covalent (metallic) bond between a 50 µm thick Al base wire and 25 µm thick Al loop wires (fig. 1) [5]. For a full-scale 1 N E-sail this bond needs to sustain a pull force of 50 mN. A multifilament tether is needed to provide micrometeoroid tolerance. Based on simulations of tether lifetime in space, a 4-wire tether structure with 3 cm long loops was manufactured.

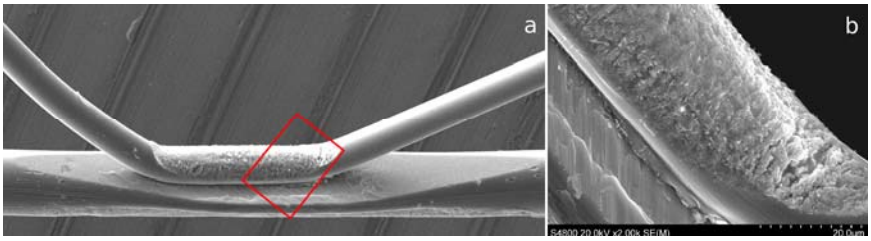

Fig. 1. Wire-to-wire bond. 25 µm diameter loop wire bonded onto a 50 µm diameter base wire (a). The base wire is automatically flattened before bonding [6]. The image on right shows the neck of the bond (b).

2. Methods

We constructed an automatic tether factory (ATF) with a machine-vision based quality assurance system. This factory is the result of in-house development during the last four years [7]. Briefly, it is built around a customized manual bonder (Kulicke & Soffa 4123) and a bonding module (fig. 2). A core part is a custom made 3-wire wedge (MicroPoint) working against a support wedge (fig. 2). The manual bonder was customized for automatic production by having an ArduinoMega 2560 control the 'manual buttons' of the bonder (fig. 3).

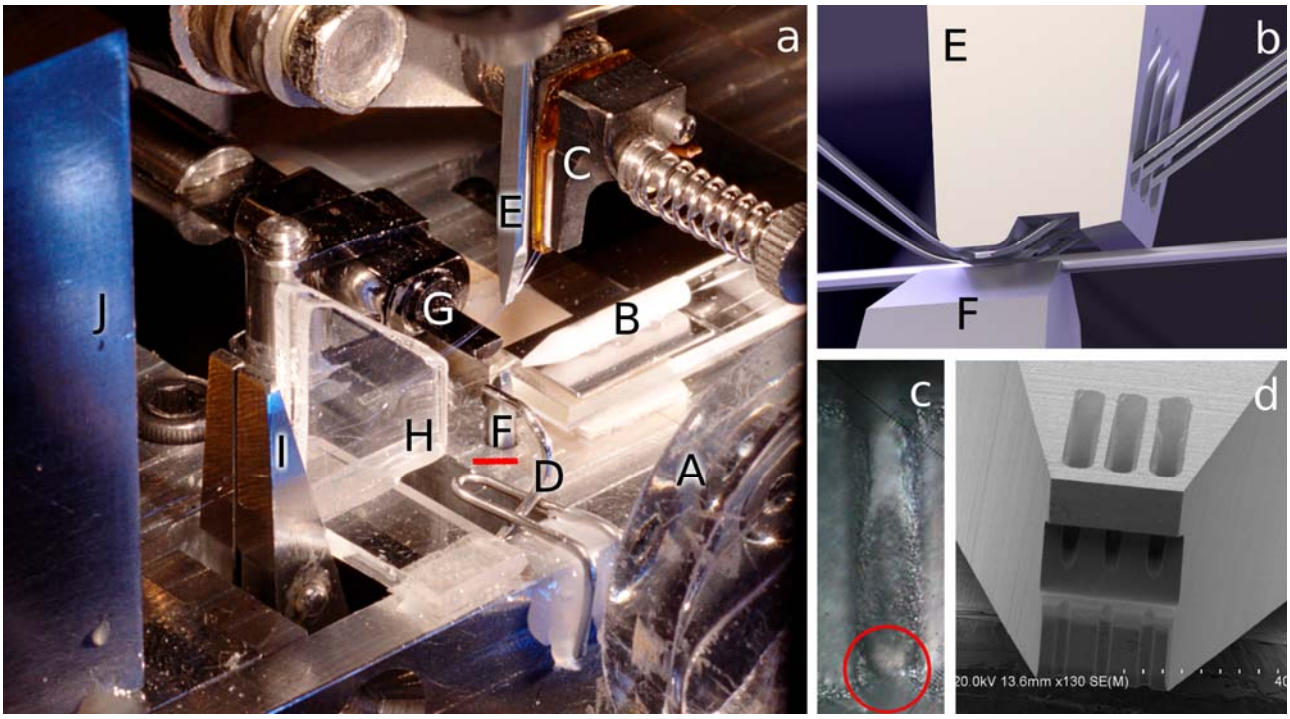

Fig. 2. (a) Tether bonding. (A) Microscope camera, (B) capillary guide for base wire, (C) clamp guide for loop wires, (D) pin for creating loops, (E) 3-wire wedge, (F) base wedge, (G) flattening tool, (H) glass guide, (I) second clamp, (J) wire guide. The red bar below F is 2 mm long. (b) Simulated image of 3-wire wedge during bonding and (d) SEM image of the 3-wire wedge. (c) Aluminum is accruing into the groove of the needle and the neck width is reduced (red circle).

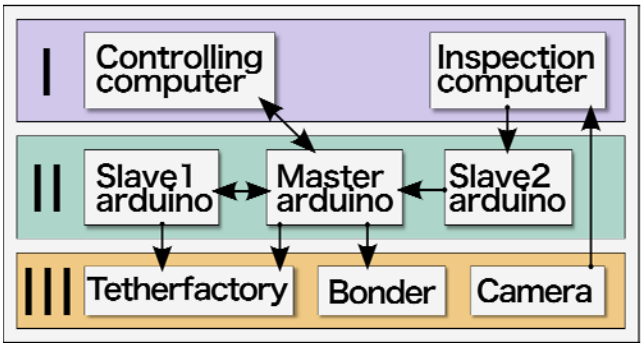

Fig. 3. ATF hardware: (layer I) PC:s, (layer II) microcontrollers, and (layer III) bonder, tether factory and camera were used in the tether production.

The core of the quality assurance system is a microscope camera (Veho VMS-004D) and a custom-made NI LabView based image acquisition software that analyzes a binarized camera image of the region of interest (ROI, fig. 4). The image analysis assures that 1) the wedge contact takes place at the correct instant of the bonding cycle, and 2) the loop wire remains in contact with the base wire after the wedge is retracted. This approach allows verifying that the loop wire adheres to the base. In

cases where this does not happen a new bond is made next to the failed one. During each wedge retraction, an image was taken, analyzed, and saved. Similarly, each operation carried out by the master Arduino was stored in a log file. In addition, the operator actions were recorded by hand.

Post production analysis to determine failure rate and types was done based on the stored images and on the computer and handwritten logs. CellProfiler [8] and R [9] softwares simplified the handling of large amounts of data during automated image analysis and data processing. Since the camera had to be repositioned due to maintenance carried out during production the images had to be reanalysed in batches where the field of view was constant. For each batch the ImageJ software [10] was used to manually find and delineate the ROI of the expected wire location between the two edges (Fig. 4). The mean intensity in the ROI was measured for all images in a batch. If the measured intensity in an image deviated by more than 4.5 sigma from the mean of the batch, the image was manually analyzed and compared to the logs.

A bond was considered ‘good’ if it remained bonded after the wedge was retracted, whereas it was considered ‘failed’ if it was either 1) lifted also after a rebonding attempt or 2) the wire was cut. A ‘repaired’ bond is a bond that was initially lifted, but later successfully rebonded next to the original spot.

Finally, we assessed how often the bonding wedge had to be cleaned to avoid reduced bond quality due to wedge fouling (fig. 2). This was done by performing post production destructive pull tests on a 97 m (9700 bonds) long tether that was produced after the main production run. This tether was produced with the same production parameters as used in the 1 km run.

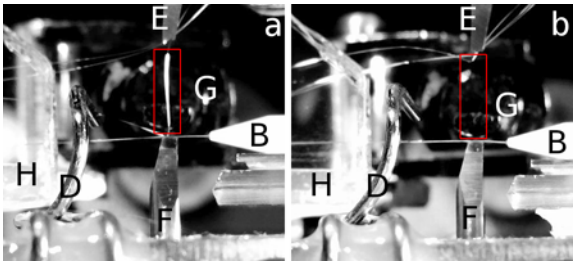

Fig. 4. Two images obtained by the quality assurance microscope camera. ‘Good’ (left) and ‘failed’ (right) bond. The red square indicates the ROI area inside which the bonding wire was searched for after the bonding process. The indicator letters correspond to those in Fig. 1.

3. Results

We produced a continuous 1.04 km long 4-wire tether that is made up of 50 µm base wire and 3 loops of 25 µm wires (fig. 6). The tether featured 90704 bonds, on average 11.5 mm apart from each other (fig. 5). The tether mass was 10 g. At the beginning of the manufacturing the measured distance between the bonds was 10 mm (3 cm loops for one loop wire). During production the distance between bonds grew to 13 mm due to tether layers accumulating on the output reel (a constant turn angle was employed).

Fig. 5. 4-wire Heytether. This sample was produced right after the 1 km production. The white bar is 10 mm long. One full loop is highlighted (red).

Fig. 6. Produced 1km tether on production reel (Tanaka AL-2 reel with additional side walls).

Production statistics are listed in table I. Seventy-four bonds remained ‘failed’ after corrective intervention had been attempted, and a loop wire was broken 8 times. In addition to tether failures, the table I also shows the number of bonds that failed in the first bonding attempt, but were automatically ‘repaired’ (successful intervention). The 195 repaired failures include 3 cases where the base wire was deliberately cut and manually repaired to practice such repairs. The failures were categorized based on the recorded logs and post production analyses of the QA images.

Table I. Produced bonds and tether failures as well as main causes of failure and ability to

recover automatically (successful intervention).

	Repaired bonds	Repaired base wire	Failed bonds	Loop wire cut	
Bond lifted	173	-	47	-	
Base wire out of groove	1	-	17	-	
Wires stuck	2	-	3	1	
Bad alignment	-	-	3	1	
Control electronic failure	6	1	1	-	
Other or unidentified*	10	2	3	6	
Total (sum)	192	3	74	8	∑ = 277 (3‰)
Repairs and failures**	∑ = 195 (2‰)		∑ = 82 (1‰)		

*Other or unidentified includes failures during manual operations. **Failures = failed bonds + loop wire cut.

Figure 7 shows the number of 'failed' and 'repaired' bonds as a function of the number of produced bonds. Initially the failure rate was higher, but between 5000 and 65000 produced bonds the failure rate remained at 0.5 ‰ (31 failures / 60.000 bonds). On average, the failure rate in the 5000 bonds produced right after wedge cleaning was 0.6 ‰ (20 failures / 7*5000 bonds). Figure 8 shows off-line tests carried out to verify that the produced tether fulfills the 50 mN tensile strength limit.

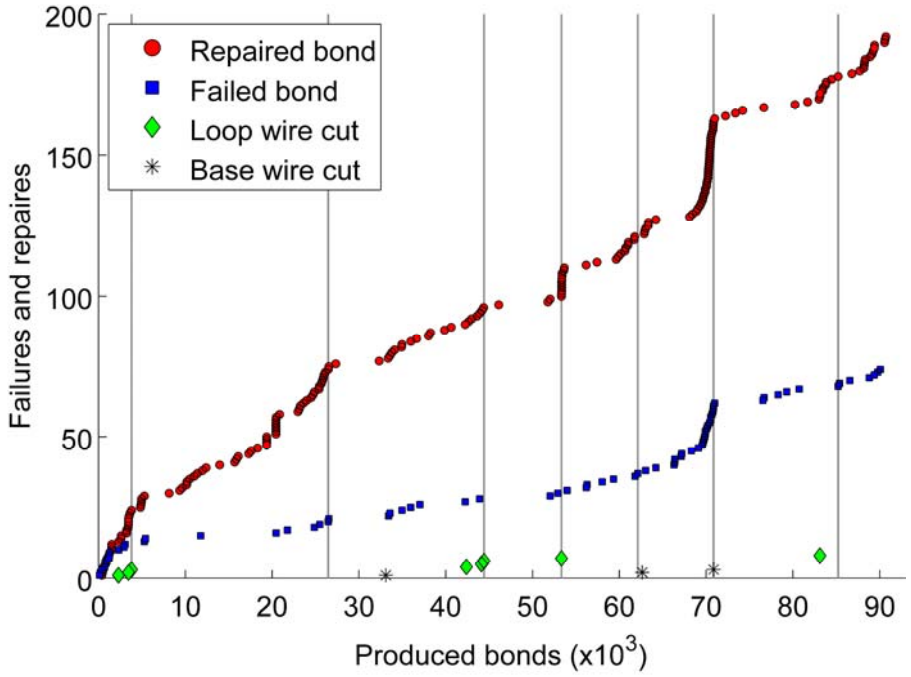

Fig. 7. Failures and repaired bonds during production as determined from the production log and image analysis. Wedge cleanings are marked by vertical lines.

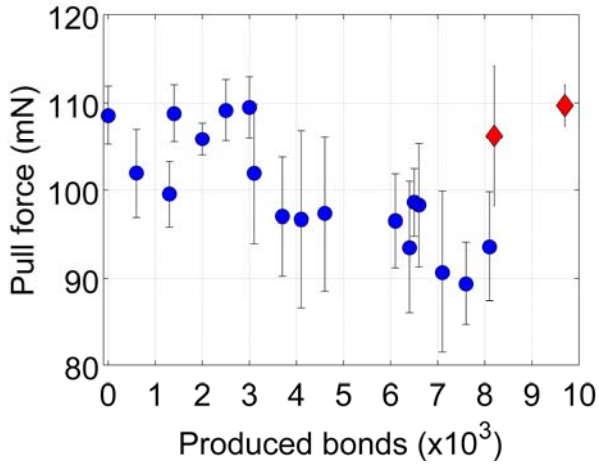

Fig. 8. Measured maximum sustainable pull force along the 97 m (9700 bonds) post production tether. The last two measurements (red) were made after wedge cleaning. Overall 252 bonds were measured. Each point comprises 6-16 measurements and the error bars indicate one standard deviation.

4. Discussion

The results indicate that a certain level of maturity in E-sail tether production has been achieved. The production is scalable and the production rate is already sufficiently high that full scale E-sails could be fabricated fast enough and economically enough to permit real-world use, by duplicating the test production line if necessary. Whereas the current production rate was 70 m/24 h, i.e. 11 sec/bond, it can in principle be improved to 400 m/day, i.e. 2 sec/bond. This estimate may be compared to the performance of commercial wirebonders that can produce more than 10 bonds/sec (wire to pad) [11]. With a 400 m/day production rate a full scale (20 km long) E-sail tether could be produced in 50 days.

The design window (what the factory can handle) is 25-150 µm for the base wire and 18-75 µm for the loop wires. This should suffice for foreseeable design requirements. The loops are currently of uniform height (<1 cm). Figure 5 reveals nicks in the loop wire caused by the 3-wire wedge. Such nicks appear in the two free loop wires when the wedge descends to bond the third wire. These nicks reduce neither tether strength nor its reelability. The slight drop in loop height caused by the nicks may reduce micrometeoroid tolerance by increasing the statistical probability that a micrometeoroid cuts both the loop wires and the base wire in one hit. In a factory employing three separately controlled wedges instead of one 3-wire wedge, smooth loops of different height could be produced independently. Variable

height loops increase the estimated life time of the tether by reducing the probability that a meteoroid cuts multiple wires by one hit.

Figure 7 shows graphically failures and repairs recorded during processing. Initially the failure rate was high due to a drift in the stepper motor that caused misalignment between the 3-wire wedge and the base wedge. The high number of failures just prior to 70000 produced bonds was caused by a problem in a clamp control. All in all (fig. 7) and table I show that the recovery (intervention) procedure reduces the number of failed bonds efficiently. We also remark that this 1 km tether production was our first attempt to make a 4-wire tether longer than 30 m.

The post production pull force data (fig. 8) show that at least 80 m continuous tether pieces can be produced without falling short of the 50 mN bond strength limit. The reason for the gradual reduction in pull force is slow accruement of Al that contaminates the grooves in the wedge (fig. 2). This contamination causes both the grip between the wire and the wedge to become less predictable and the wire at the neck of the bond to become weaker (fig. 1). Both issues reduce the pull force and contribute to instability of the bonding process (fig. 8). The number of produced bonds between interventions may be increased by further optimization of the 3-wire and base wedge designs as well as by optimizing the bonding parameters. The tether quality is currently assessed inline on a binary scale (‘good’ / ‘failed’). In principle it should be possible to determine the tether quality more precisely using image analysis [12], contact resistance [13] or ultrasonics [14]. We believe that a nondestructive online method for measuring tether quality is necessary in future tether factories to ensure consistent and verifiable quality of up to 20 km long tethers.

From a mechanical point of view, the E-sail tether needs to sustain micrometeoroids, centrifugal tension during operation, reeling in at the factory, launch vibrations, and reeling out in space. These factors affect the choice of tether shape, wire materials, and production technique. The multifilament Heytether with one base wire and three loop wires was selected because of its micrometeoroid tolerance, reelability, producability and weight/strength ratio. The current Heytether tolerates a situation where two loop wires and the base wire is cut by a micrometeoroid. The probability of tolerating micrometeoroids is further improved by producing taller loops of different heights because it reduces the probability that a micrometeoroid cuts more than one wire by one hit. The weight/strength ratio of the tether is an important

design parameter for the full scale E-sail. The tether strength is defined by its weakest points, the wire-to-wire bonds. Figure 8 shows that bonds stronger than 50 mN can be produced, but to ensure that production drifts are accommodated and that single failures occur much below the 1% limit (relative fraction of failed bonds), real-time quality control [15] may be needed. The quality control method should without contact directly measure the maximum sustainable pull force of the bonds because the bonds generally the weakest points of the tether. Whereas this study shows that Heytether on large scale can be produced, the reeling in and out operations still need to be optimized and tested.

5. Conclusions

We produced a 1 km continuous piece of space qualified E-sail tether. We reached a production rate of 70 m/24 hours and a quality level of 0.1‰ loose bonds. The tether comprising 90704 bonds was reeled onto a reel compatible with CubeSats. This result demonstrates that large scale production of E-sail tether is possible and practical.

References

[1] P. Janhunen, "Electric sail for spacecraft propulsion," *Journal of Propulsion and Power*, vol. 20, no. 4, p. 763, 2004.

[2] P. Janhunen, P. K. Toivanen, J. Polkko, S. Merikallio, P. Salminen, E. Hæggström, H. Seppänen, R. Kurppa, J. Ukkonen, S. Kiprich, G. Thornell, H. Kratz, L. Richter, O. Krömer, R. Rosta, M. Noorma, J. Envall, S. Lätt, G. Mengali, A. A. Quarta, H. Koivisto, O. Tarvainen, T. Kalvas, J. Kauppinen, A. Nuottajärvi, and A. Obraztsov, "Invited Article: Electric solar wind sail: Toward test missions," *Rev. Sci. Instrum.*, vol. 81, no. 11, p. 111301, 2010.

[3] A. A. Quarta and G. Mengali, "Electric Sail Mission Analysis for Outer Solar System Exploration," *Journal of Guidance, Control, and Dynamics*, vol. 33, no. 3, pp. 740–755, May 2010.

[4] G. Mengali and A. A. Quarta, "Non-Keplerian orbits for electric sails," *Celestial Mechanics and Dynamical Astronomy*, vol. 105, no. 1–3, pp. 179–195, Mar. 2009.

[5] H. Seppänen, S. Kiprich, R. Kurppa, P. Janhunen, and E. Hæggström, "Wire-to-wire bonding of μm-diameter aluminum wires for the Electric Solar Wind Sail," *Microelectronic Engineering*, vol. 88, no. 11, pp. 3267–3269, Nov. 2011.

[6] Henri Seppänen, Sergiy Kiprich, Risto Kurppa, Jukka Ukkonen, Tuomo Ylitalo, Pekka Janhunen, and Edward Hæggström, "Multifilament Tether for Electric Solar Wind Sail," presented at the IMAPS Workshop on Wire Bonding, San Francisco Marriott Hotel, San Francisco, CA, 2011.

[7] Timo Rauhala, Henri Seppänen, Jukka Ukkonen, Sergiy Kiprich, Göran Maconi, Pekka Janhunen, and Edward Hæggström, "Automatic 4-wire Heytether production for the Electric Solar Wind Sail," presented at the Wire Bonding Workshop, Radisson Hotel San Jose Airport San Jose, CA 95112, 2013.

[8] A. E. Carpenter, T. R. Jones, M. R. Lamprecht, C. Clarke, I. H. Kang, O. Friman, D. A. Guertin, J. H. Chang, R. A. Lindquist, J. Moffat, P. Golland, and D. M. Sabatini, "CellProfiler: image analysis software for identifying and quantifying cell phenotypes,"

Genome Biol., vol. 7, no. 10, p. R100, 2006.
[9] *R Core Team (2012). R: A language and environment for statistical computing. R Foundation for Statistical Computing, Vienna, Austria. ISBN 3-900051-07-0, URL http://www.R-project.org/.* .
[10] C. A. Schneider, W. S. Rasband, and K. W. Eliceiri, "NIH Image to ImageJ: 25 years of image analysis," *Nat Meth*, vol. 9, no. 7, pp. 671–675, Jul. 2012.
[11] "High Speed Fully Automatic Fine Wire Wedge Bonder (Bondjet BJ820), Retrieved March 26, 2013 from http://www.hesse-mechatronics.com." .
[12] H. Seppänen, R. Schäfer, I. Kassamakov, P. Hauptmann, and E. Hæggström, "Automated optical method for ultrasonic bond pull force estimation," *Microelectronic Engineering*, vol. 87, no. 9, pp. 1796–1804, Nov. 2010.
[13] H. Seppänen, R. Kurppa, A. Meriläinen, and E. Hæggström, "Real time contact resistance measurement to determine when microwelds start to form during ultrasonic wire bonding," *Microelectronic Engineering*, vol. 104, pp. 114–119, Apr. 2013.
[14] H. Gaul, M. Schneider-Ramelow, K. D. Lang, and H. Reichl, "Predicting the Shear Strength of a Wire Bond Using Laser Vibration Measurements," in *Electronics Systemintegration Technology Conference, 2006. 1st*, 2006, vol. 2, pp. 719–725.
[15] M. Brokelmann, J. Wallaschek, and H. Hesse, "Bond process monitoring via self-sensing piezoelectric transducers," in *Frequency Control Symposium and Exposition, 2004. Proceedings of the 2004 IEEE International*, 2004, pp. 125–129.